Compartmentalization of Reverse Atom Transfer Radical Polymerization in Miniemulsion

Ryan W. Simms and Michael F. Cunningham*

Department of Chemical Engineering, Queen's University, Kingston, Ontario, Canada K7L 3N6

Received February 21, 2008; Revised Manuscript Received May 12, 2008

ABSTRACT: Compartmentalization of an atom transfer radical polymerization (ATRP) miniemulsion has been experimentally observed to reduce the overall polymerization rate, primarily by increasing the rate of deactivation due to the confined space effect, and compartmentalization was also found to improve the control over the polymerization and to reduce the final polydispersity index of the polymer. Compartmentalization of an ATRP system requires that the probability of having two active chains in one particle becomes sufficiently low that the particle size influences the number of active radicals (through segregation and confined space effects). This probability is determined by both the particle volume and the number of polymer chains within each particle. For a given number of chains, compartmentalization effects become evident only when the number of reactants (active polymeric radicals and the deactivating species $CuBr_2$−tris[2-di(2-ethylhexyl acrylate)aminoethyl]amine (EHA_6TREN)) within each particle becomes limited by decreasing particle volume. Alternatively, for a given particle volume compartmentalization effects become evident when reactants (active polymeric radicals and the deactivating species $CuBr_2$−EHA_6TREN) become limited by decreasing chain number. The difference between a conventional free radical polymerization and ATRP is highlighted by the opposing impact that compartmentalization has on the kinetics of the polymerizations. In a conventional system, segregation effects cause an increase in the polymerization rate, while the confined space effect dominates the kinetics in ATRP and results in a decrease in rate.

Introduction

Progress in living/controlled radical polymerization (L/CRP) conducted in aqueous-based systems has highlighted the significant differences of L/CRP conducted in bulk vs (mini)emulsion and between conventional free radical (mini)emulsion and L/CRP (mini)emulsion systems. To effectively perform an aqueous-based L/CRP, it is important to determine the suitability of the controlling species and initiator (phase partitioning, stability) and the potential influence of the L/CRP mechanism on the kinetics of the polymerization, particle nucleation, radical entry and exit from the particle, and stability of the latex.[1–3] For L/CRP based on the reversible termination mechanism of control, atom transfer radical polymerization (ATRP),[4–12] and nitroxide-mediated polymerization (NMP),[13–18] a complete understanding of the kinetics has been concealed by the complexity of the system. Most notable among the poorly understood kinetic issues is whether conducting ATRP/NMP in a small reaction volume can result in compartmentalization and to what extent it influences the system.

Compartmentalization in a conventional free radical (mini)-emulsion polymerization increases the rate of polymerization and the molecular weight of the polymer compared to its bulk counterpart. This is a consequence of the segregation effect of compartmentalization, in which radicals in different particles are unable to mutually terminate, decreasing the termination rate and therefore increasing the overall polymerization rate of the system. Another important aspect of compartmentalization is the confined space effect, where the reaction rate between two radicals in the same particle increases with decreasing particle volume (the basis of "zero-one" kinetics in emulsion polymerization).[19]

Under the right conditions compartmentalization has been observed in L/CRP based on reversible transfer reactions (reversible addition fragmentation transfer (RAFT) and macromolecular design via interchange of xanthates (MADIX)) by an increase in the polymerization rate with decreasing particle size.[20–24] The influence of compartmentalization in RAFT/MADIX is similar to a conventional free radical polymerization because of the mechanistic similarity of the two techniques. The mechanism of control in an ideal RAFT/MADIX process maintains the same population of free radicals as the conventional free radical polymerization, and both techniques involve the steady release of primary radicals from an initiator source for the duration of the polymerization. Therefore, under the right conditions, small reaction volumes in a RAFT/MADIX system result in segregated propagating radicals, leading to the reduced termination of propagating polymer chains and an increase in the overall polymerization rate.

While compartmentalization is present in RAFT/MADIX, it has been generally accepted that for reversible termination systems (ATRP/NMP) compartmentalization does not exist due to the method of controlling the polymerization in these techniques. The polymer chains are reversibly terminated through repeated activation/deactivation cycles, with the vast majority of chains being in the dormant state at any one time. Compared to a conventional free radical polymerization, the probability of mutual termination in ATRP is kept to a minimum because the concentration of active radical species is maintained at a very low level, dictated by the ATRP equilibrium (determined by the ATRP equilibrium constant K_{eq}, eq 1) that is established in the system. Also unique to ATRP (and NMP) is that after the initiation period at the start of the polymerization (in which all the polymer chains are formed) there are no primary (short chain) radicals in the system (excluding transfer reactions and thermally generated radicals) so that radical entry and exit are of minimal importance. Therefore, ATRP should behave as a pseudobulk system because the very low concentration of active radicals coupled with no short chain radicals (entry/exit effects) means that the size of the particle should not influence the polymerization.

* To whom correspondence should be addressed. E-mail: michael.cunningham@chee.queensu.ca.

10.1021/ma8003967 CCC: $40.75
Published on Web 06/21/2008

$$K_{eq} = \frac{[\text{active radicals}][\text{deactivator}]}{[\text{dormant chains}][\text{activator}]} = \frac{[P^{\bullet}][Cu(II)]}{[\text{dormant chains}][Cu(I)]} \quad (1)$$

A limited number of modeling studies of NMP suggest that under the right set of conditions compartmentalization may occur, although all of the reported effects on system do not agree. Charleux considered the segregation of propagating radicals, using a Smith-Ewart approach for the model that predicted faster rates of polymerization for smaller particle sizes.[25] Butte et al.[26] accounted for the segregation of the nitroxide as well as the propagating radicals and concluded that the polymerization rate would decrease in smaller particles, which has since been expanded on by Zetterlund and Okubo.[27] Experimental results have shown that the size of the particle can influence NMP in miniemulsion through interfacial effects.[28] Recently, experimental evidence for compartmentalization in miniemulsion NMP was reported by Maehata et al.,[29] who found that decreasing particle size resulted in lower rates of polymerization and superior livingness of the polymer chains in 2,2,6,6-tetramethylpiperidinyl-1-oxy (TEMPO)-mediated styrene polymerization. However, Delaittre and Charleux reported that no compartmentalization effects were seen in the formation of poly(acrylic acid)-*b*-polystyrene amphiphilic block copolymers by *N*-*tert*-butyl-*N*-(1-diethylphosphono-2,2-dimethylpropyl) nitroxide (SG1)-mediated emulsion polymerization.[30] It was proposed that SG1 could not be compartmentalized since it can rapidly diffuse throughout the system.

A theoretical study on the compartmentalization of ATRP predicted that at sufficiently small particle sizes compartmentalization should cause a decrease in the polymer chain termination rate and an increase in the ATRP deactivation rate, leading to better control and slower polymerization rates.[31] The present paper provides the first experimental evidence for compartmentalization in miniemulsion ATRP through observed particle size affects on the rate of polymerization and the degree of control over the polymerization.

Experimental Section

Materials. *n*-Butyl methacrylate (BMA, 99%, Aldrich) and 2-ethylhexyl acrylate (98%, Aldrich) were purified by passing them through a column packed with inhibitor remover (Aldrich). Copper(II) bromide ($CuBr_2$, 99%, Aldrich), tris(2-aminoethyl)amine (96%, Aldrich), cetyltrimethylammonium bromide (CTAB, Aldrich), hexadecane (99%, Aldrich), ascorbic acid (AA, 99%, Aldrich), hydrogen peroxide (3 wt % in water, Aldrich), basic alumina (Aldrich), and 2,2′-azobis[2-(2-imidazolin-2-yl)propane] dihydrochloride (VA-044, Wako Chemicals) were used as received. The synthesis of tris[2-di(2-ethylhexyl acrylate)aminoethyl]amine (EHA_6TREN) was adapted from literature methods.[32,33]

Miniemulsion Polymerization. In a typical experiment, the organic phase was prepared by adding $CuBr_2$ (0.0766 g, 3.43×10^{-4} mol), EHA_6TREN (0.440 g, 3.51×10^{-4} mol), hexadecane (1.48 g, 3.8 wt % vs monomer), and BMA (39.0 g, 0.274 mol, 15 wt % vs deionized water) to a beaker and stirring overnight at room temperature to form a homogeneous solution. The aqueous phase, which consisted of the surfactant CTAB (1.17 g, 3 wt % vs BMA) and deionized water (221 g), was stirred overnight at room temperature. The organic phase was added to the surfactant solution and stirred for ~30 min prior to passing through a Microfluidizer 110S (Microfluidics International Corp.) operating at an inlet pressure of 275 kPa. The miniemulsion (200 g) was transferred to a 500 mL round-bottom flask fitted with a condenser and was purged with ultrahigh-purity nitrogen for 30 min before being immersed in a 90 °C oil bath with the magnetic stirring speed set to 250 rpm. Fifteen minutes elapsed before the addition on the initiator. The AA (0.0143 g, 1.65×10^{-4} mol) and hydrogen peroxide (0.188 g of 3 wt % hydrogen peroxide, 8.12×10^{-5} mol) were added to separate Schlenk tubes, mixed with 2 mL of deionized water, and purged with ultrahigh-purity nitrogen for 20 min prior to injection. Using a deoxygenated syringe, the hydrogen peroxide was added prior to the AA, which was added dropwise over 5 min. Samples were withdrawn with a deoxygenated syringe and placed in an ice bath.

Characterization. After the polymerizations were complete, the latexes were filtered (Fisherbrand P8 creped) to collect any coagulum. The amount of coagulum was determined gravimetrically (all experiments had less than 2 wt % coagulum). Monomer conversions were determined gravimetrically. Size exclusion chromatography (SEC) was used to measure the molecular weight distribution of the polymer samples. The dried polymer samples from the miniemulsion were dissolved in tetrahydrofuran (THF) and passed through a column packed with basic alumina to remove the residual copper. The SEC was equipped with a Waters 2960 separation module containing four Styragel columns (100, 500, 10^3, and 10^4 Å) maintained at 40 °C, coupled with a Waters 410 differential refractive index detector and a Wyatt Technology DAWN EOS photometer multiangle light scattering (LS) detector (690 nm, 30 mW Ga−As laser). THF was used as the eluant, and the flow rate was set to 1.0 mL min^{-1}. The LS detector was calibrated with toluene and normalized with a 30 000 g mol^{-1} narrow polystyrene standard. Data were processed using Astra (version 4.90.08) software. A d*n*/d*c* value of 0.075 was used for poly(butyl methacrylate) (PBMA).[34] Particle sizes of the latexes were measured using a Matec Applied Sciences capillary hydrodynamic fractionation (CHDF) 2000 unit. The UV detector was set to 220 nm. The eluant was a 20:1 mixture of deionized water/GR500-1X (Matec Applied Sciences). Samples were diluted with the eluant to ~3.5 wt % solids and sonicated for 5 min. Samples were passed through a 0.5 μm pore size filter prior to injection. The marker was a 2 wt % solution of sodium benzoate. To ensure that there were no particles greater than 0.5 μm, the particle size distributions were also measured using a Malvern Mastersizer 2000 equipped with a Hydro 2000S optical unit. The refractive index value for water and PBMA were 1.33 and 1.48, respectively.

Determining the Number of Radicals. The average number of free radicals per latex particle ($\bar{n}$) was calculated at ~30% conversion from the observed polymerization rate (as d(fractional conversion)/d*t*, d*x*/d*t*) and the calculated value of monomer concentration [M] using the rate equation for an emulsion polymerization (eq 2).[19]

$$dx/dt = k_p[M]\bar{n}N_c/n_M^0N_A \quad (2)$$

n_M^0 is the initial number of moles of monomer present, N_c is the number concentration of particles, N_A is Avogadro's constant, and the propagation rate coefficient k_p was calculated from eq 3:[35]

$$k_p = 10^{6.58}\exp(-22.9/RT) \quad (3)$$

While $\bar{n}$ is an informative parameter that can be used to illustrate compartmentalization in conventional free radical emulsion polymerization, it can be misleading when applied to ATRP. This is because for ATRP the number of active radicals is dictated by the ATRP equilibrium and is a function of the number of polymer chains present (eq 1). For example, doubling the volume of a particle would cause a 2-fold increase in the number of polymer chains per particle (N_{chain}), and as a consequence, the value of $\bar{n}$ would also be doubled. To account for this effect, (i.e., that the number of free radicals in each particle is a function of the number of polymer chains), $\bar{n}$ has been normalized against the number of polymer chains. The average number of radicals per particle per polymer chain ($\bar{n}_{chain}$) was calculated using eq 4.

$$\bar{n}_{chain} = \bar{n}/N_{chain} \quad (4)$$

Results and Discussion

Effect of Particle Size on Miniemulsion ATRP. The polymerization of BMA was carried out in miniemulsion using an ATRP process, mediated with $CuBr_2$−EHA_6TREN, and

Table 1. Summary of Experiments for the Reverse Atom Transfer Radical Polymerization of Butyl Methacrylate (BMA) in Miniemulsion[a] at 90 °C Initiated with the Redox Pair Hydrogen Peroxide/Ascorbic Acid (AA) and Stabilized with Cetyltrimethylammonium Bromide (CTAB)

expt	CTAB (wt %)[b]	$[BMA]_0/[CuBr_2]_0/[hydrogen\ peroxide]_0/[AA]_0$	conv[c] (%)	M_n[d] (kg mol^{-1})	PDI[e]	D_p[f] (nm)	SD[g]	k_{app}[h] ($s^{-1} \times 10^{-5}$)	N_c[i] ($\times 10^{-16}$)	$\bar{n}$[j] ($\times 10^3$)	N_{chain}[k] ($\times 10^{-2}$)	$\bar{n}_{chain}$[l] ($\times 10^6$)
1	0.5	1270:1.6:1:0.5	69	505	1.52	212	94	17.2	3.5	59.1	41.4	12.2
2	1.0	1270:1.6:1:0.5	85	644	1.29	176	48	19.2	6.0	24.2	23.6	10.3
3	2.0	1270:1.6:1:0.5	81	601	1.20	142	50	9.7	11.4	5.7	12.6	4.5
4	2.0 + 1.0[m]	1270:1.6:1:0.5	73	511	1.21	141	16	9.5	11.8	5.1	12.7	4.0
5	3.0	1270:1.6:1:0.5	68	496	1.19	119	16	5.0	20.0	2.0	7.3	2.7
6	1.0	1270:1.3:1:0.5	84	606	1.27	162	34	23.3	7.7	25.8	19.2	13.5
7	1.0	1270:1.0:1:0.5	82	584	1.49	159	36	29.2	8.1	24.5	18.5	13.3
8	3.0	1270:1.3:1:0.5	85	684	1.18	116	22	11.3	20.1	3.6	6.3	5.6
9	3.0	1270:1.0:1:0.5	79	652	1.21	119	26	17.3	19.5	9.1	6.6	13.7
10	1.0	630:1.6:1:0.5	87	438	1.42	172	67	20.5	6.4	22.4	33.1	6.8
11	2.0	630:1.6:1:0.5	89	441	1.31	147	60	16.1	10.1	12.2	21.0	5.8
12	3.0	630:1.6:1:0.5	84	400	1.18	130	28	14.0	12.0	6.7	15.0	4.5
13	1.0	1590:1.6:1:0.5	75	559	1.33	155	38	13.0	8.7	15.6	16.4	9.5
14	2.0	1590:1.6:1:0.5	77	711	1.20	131	27	7.8	14.7	5.5	7.8	7.1
15	3.0	1590:1.6:1:0.5	69	658	1.18	117	22	5.4	20.1	2.3	5.4	4.3
16	2.5	400:1.0:0.32[n]	84	92.0	1.32	146	25	20.7	10.4	19.5	93.5	2.1
17	0.5	400:1.0:0.32[n]	79	95.2	1.35	196	45	21.7	4.4	44.8	202.3	2.3

[a] [Hexadecane] = 3.8 wt % based on total monomer; 15% solid content. [b] Based on total monomer. [c] conv = conversion, determined gravimetrically. [d] M_n = number-average molecular weight, determined from size exclusion chromatography. [e] PDI = polydispersity index, determined from size exclusion chromatography. [f] D_p = weight-average particle diameter, determined with capillary hydrodynamic fractionation. [g] SD = standard deviation of the weight-average particle diameter, determined with capillary hydrodynamic fractionation. [h] k^{app} = apparent rate constant. [i] N_c = number concentration (number density) of particles (= $(V_{total\ organic}/V_{particle})/V_{aq}$ (particles L_{water}^{-1})). [j] $\bar{n}$ = average number of radicals per latex particle (L_{water}^{-1}). [k] N_{chain} = average number of polymer chains per latex particle (= $(N_A mass_{polymer}/M_n)/(N_c V_{aq})$). [l] $\bar{n}_{chain}$ = average number of radicals per polymer chain (chain^{-1} L_{water}^{-1}). [m] After passing the solution through the microfluidizer to form the miniemulsion another 1 wt % CTAB was added to the system. [n] Initiated with the azo compound 2,2′-azobis[2-(2-imidazolin-2-yl)propane] dihydrochloride (VA-044).

initiated by the redox pair hydrogen peroxide/AA. The highly hydrophobic ligand EHA_6TREN was selected to minimize the water solubility of the copper species. With the copper species sequestered in the droplets/particles the influence of their compartmentalization on the system could be observed experimentally. Previous work with this system produced high number-average molecular weight (M_n) polymers (up to $M_n \sim 1\,000\,000$ g mol^{-1}) with a narrow polydispersity index (PDI < 1.25) at relatively fast rates of polymerization (compared to typical ATRP systems).[34] In the present investigation, the effect of particle diameter (D_p) on the system was studied by varying the surfactant loading from 0.5 to 3 wt % based on monomer. The cationic surfactant CTAB was used in all experiments. Table 1 provides a summary of the essential experimental conditions and results.

In experiments 1−5 the effect of surfactant loading was investigated on identically formulated systems ($[BMA]_0/[CuBr_2$-$EHA_6TREN]_0/[hydrogen\ peroxide]_0/[AA]_0 = 1270:1.6:1.0:0.5$). There is a clear trend between the amount of surfactant and the D_p of the final latex (Table 1), ranging from 212 nm (experiment 1, 0.5 wt % CTAB) to 119 nm (experiment 5, 3 wt % CTAB).

Figure 1a plots M_n vs conversion, which illustrates the linear increase in the molecular weight with conversion, and shows that the CTAB loading has no discernible effect on the molecular weight of the polymer (or on the number of polymer chains generated) since the evolution of M_n with conversion is consistent between experiments. The one exception is experiment 1, with a surfactant loading of 0.5 wt % CTAB, which has a lower M_n until about 60% conversion at which point there is an increase in M_n, where it then attains the same value as experiments 2−5. The poor control of the polymerization in experiment 1 is also evident in the PDI vs conversion plot (Figure 1b). The PDI reaches a minimum value of 1.39 at ∼31% conversion and then increases with conversion, reaching a value greater than 1.6 before ending at ∼1.5. For experiments 2−5 the PDI has the expected trend for a well-controlled polymerization, which is to continually decrease with conversion (final PDI ∼ 1.25). The poor control of the polymerization in experiment 1 is believed to result from a decreased influence of compartmentalization due to the large D_p for the system. This will be elaborated on later in the text.

It is evident from the conversion vs time plots shown in Figure 1c that there is a trend of decreasing polymerization rate (R_p) with increased CTAB loading (decreasing particle size). Modeling of the basic reverse ATRP mechanism for solution/bulk systems, for which heterogeneous systems have typically adhered to, leads to the R_p defined in eq 5.[36−38]

$$R_p = k_p[M][P^\bullet] = k_p[M]K_{eq}[\text{dormant chain}][Cu(I)]/[Cu(II)] = k^{app}[M] \quad (5)$$

$$\ln([M]_0/[M]) = k^{app}t \quad (6)$$

From eq 5 it is expected that the R_p should be consistent between the identically formulated experiments because k_p, [M], K_{eq}, [Cu(II)], and [Cu(I)] are constant between the experiments. As well, the evolution of M_n with conversion is similar between the experiments, from which it is determined that the concentration of "living" polymer chains ([living chains] = [dormant chain] + [active chains] ≈ [dormant chains]) is constant among the experiments. The polymerization rates for this investigation are quantified with the apparent rate constant (k^{app}, eq 6, Table 1), which has a range of $12.3 \times 10^5 - 5.0 \times 10^5$ s^{-1} for a CTAB loading of 0.5 and 3 wt %, respectively.

Experiment 4 was run to ensure that the effects on the polymerization were due to the variation in D_p and not an unknown interaction with CTAB. The conditions were identical to experiment 3; however, after passing the solution through the microfluidizer to form the miniemulsion, an additional 1 wt % CTAB was added to the system. This produced a similar D_p for experiment 3 (142 nm) and experiment 4 (141 nm) but with different CTAB loadings of 2 and 3 wt %, respectively. As seen in Figure 1 and Table 1, the behavior of experiments 3 and 4 are comparable, affirming that it is the D_p influencing the behavior of the polymerization.

In a conventional (mini)emulsion polymerization, compartmentalization causes segregation and confined space effects that result from the amount of a reactant(s) being limited by the volume of the particle. For ATRP to exhibit compartmentalization effects the concentrations of the active polymeric radical and/or the persistent radical ($CuBr_2-EHA_6TREN$) will need to be restricted by the particle volume, thereby resulting in different

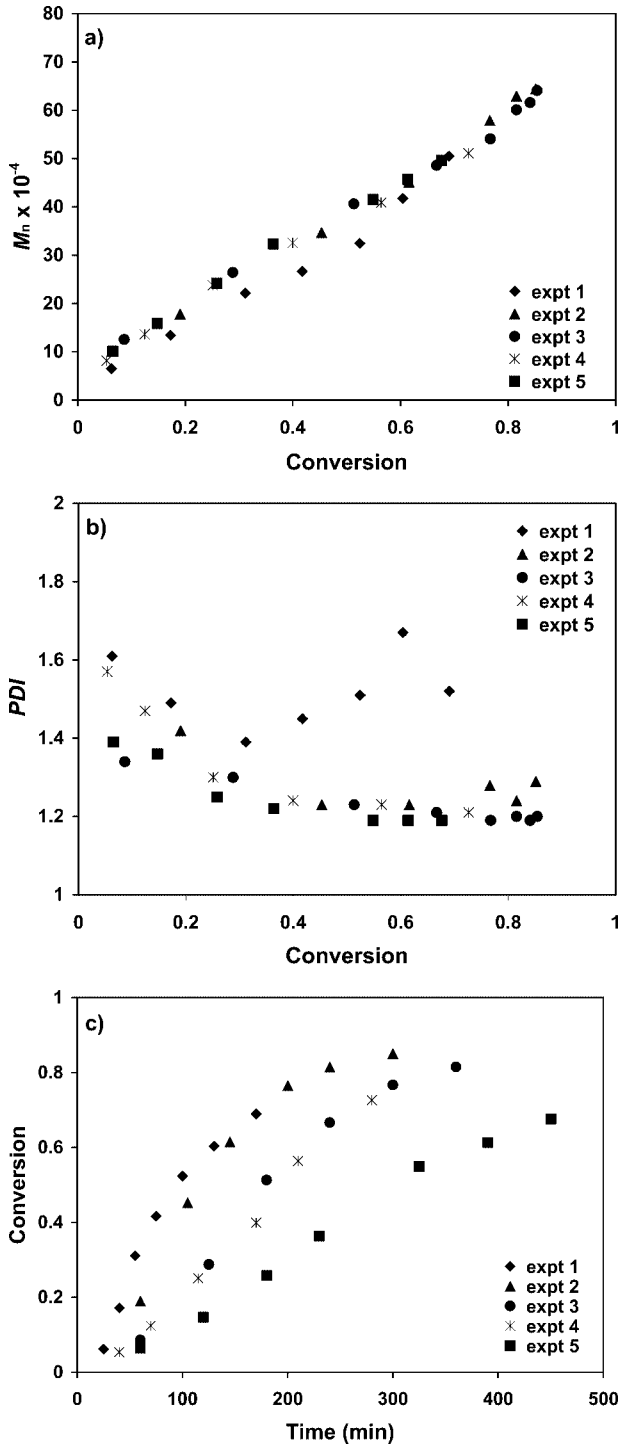

Figure 1. Evolution of (a) number-average molecular weight (M_n) and (b) polydispersity index (PDI) with conversion and (c) conversion vs time plots for the reverse atom transfer radical polymerization of butyl methacrylate (BMA) at 90 °C in miniemulsion with varying amounts of cetyltrimethylammonium bromide (CTAB). 15% solid content; [hexadecane] = 3.8 wt % based on monomer; $[BMA]_0/[copper(II)$ bromide tris[2-di(2-ethylhexyl acrylate)aminoethyl]amine/[hydrogen peroxide/[ascorbic acid = 1270:1.6:1:0.5; expt 1: 0.5 wt % CTAB; expt 2: 1 wt % CTAB; expt 3: 2 wt % CTAB; expt 4: 2 + 1 wt % CTAB; expt 5: 3 wt % CTAB.

behavior (rate, molecular weight distribution, livingness) than would be observed in a similar bulk system. The use of the initiation system hydrogen peroxide/AA, in experiments 2−5, produces polymers with high M_n (∼600 000 g mol^{-1} at 80% conversion), resulting in a range of N_{chain} from 2360 (expt 2) to 730 (expt 5) chains/particle. (By comparison, typical L/CRP miniemulsions yielding lower molecular weight polymers have $>\sim 10^4$ chains/particle.) The low concentration ofpolymer chains would limit the availability of both the active polymeric radicals and $CuBr_2-EHA_6TREN$, thereby reducing the probability of having two active radicals in the same particle. To illustrate that the number of active radicals in the system is influenced by the size of the particle, the value of $\bar{n}_{chain}$ was calculated using eq 4, and the data are summarized in Table 1. Excluding experiment 1 (due to its poor control), there is a trend of decreasing $\bar{n}_{chain}$ with D_p from experiment 2 ($\bar{n}_{chain} = 10.3 \times 10^{-6}$ L_{water}^{-1} chain^{-1}, $D_p = 176$ nm) through experiment 5 ($\bar{n}_{chain} = 2.7 \times 10^{-6}$ L_{water}^{-1} chain^{-1}, $D_p = 119$ nm). As will be seen in the subsequent discussion, the decrease in $\bar{n}_{chain}$ (and subsequently k^{app}) with decreasing D_p is likely caused by the confined space effect, which increases the reaction rate between an active polymeric radical and $CuBr_2-EHA_6TREN$ when the reaction volume is decreased.

Previously, compartmentalization has not been seen in miniemulsion ATRP because the large number polymer chains in each particle meant that each particle operated as a "nanoreactor", where the reaction kinetics in the particle are identical to a bulk system. To show that in a noncompartmentalized system k^{app} and $\bar{n}_{chain}$ are independent of D_p, we analyzed data from a previous study of miniemulsion ATRP in which compartmentalization was not present.[12] Experiments 16 and 17 in Table 1 summarize the results of earlier work on a very similar system in which the azo-initiator VA-044 was used instead of hydrogen peroxide/AA. With the exception of varying the amount of CTAB, the experiments were run under identical conditions with $[BMA]_0/[CuBr_2-EHA_6TREN]_0/[VA\text{-}044]_0$ = 400:1:0.32. The M_n reached a value of ∼90 000 g mol^{-1} at 80% conversion and increased linearly with conversion while the PDI decreased with conversion, reaching a final value less than 1.35. In spite of the difference in the particle size, the k^{app} and $\bar{n}_{chain}$ were similar for experiment 16 (2.5 wt % CTAB, $D_p = 146$ nm, $k^{app} = 20.7 \times 10^5$ s^{-1}, $\bar{n}_{chain} = 2.1 \times 10^{-6}$ L_{water}^{-1} chain^{-1}) and experiment 17 (0.5 wt % CTAB, $D_p = 196$ nm, $k^{app} = 21.7 \times 10^5$ s^{-1}, $\bar{n}_{chain} = 2.3 \times 10^{-6}$ L_{water}^{-1} chain^{-1}), indicating the absence of any compartmentalization effects. This analysis also highlights the benefit of using $\bar{n}_{chain}$ as a metric; it can be seen in Table 1 that the value of $\bar{n}$ in experiment 17 was calculated to be more than twice that of experiment 16, but this is primarily the result of having more than double the number of polymer chains in each particle in experiment 17. In experiments 16 and 17, the relatively high value for N_{chain} and the subsequently high concentration of active polymeric radicals and $CuBr_2-EHA_6TREN$ meant that varying the particles size did not influence the number of active radicals in the system, which were controlled solely by the ATRP equilibrium.

The second important aspect of compartmentalization is the segregation of radical species limiting the occurrence of mutual termination. This would be expected to increase the rate of polymerization because the number of living chains would remain at its maximum and the buildup of the deactivating species $CuBr_2-EHA_6TREN$ due to termination reactions would be minimized (eq 5). However, the large decrease in the k^{app} with decreasing D_p observed experimentally shows that the effect of radical segregation on the kinetics is eclipsed by the confined space effect previously discussed. Radical segregation could also manifest itself through improved control of the polymerization (due to reduced termination), which would be seen experimentally as a decrease in the PDI of the polymer. (The increased rate of deactivation from the confined space effect would increase the number of activation/deactivation cycles the polymer chains would undergo, also contributing to a lower PDI.) A comparison of experiments 1 and 2 clearly depicts the influence that compartmentalization can have on the

control of the polymerization. The poorly controlled polymerization in experiment 1 had a D_p of 212 nm, which contained an average of 4140 polymer chains per particle with an $\bar{n}_{chain}$ value of 12.2×10^{-6} L_{water}^{-1} $chain^{-1}$, resulting in an M_n that did not grown linearly with conversion and a final PDI of 1.52. The D_p in experiment 2 of 176 nm produces a particle with roughly half the volume of experiment 1, containing an average of 2360 chains per particle with an $\bar{n}_{chain}$ value of 10.3×10^{-6} L_{water}^{-1} $chain^{-1}$; the well-controlled polymerization had a final PDI of 1.29. The trend of decreasing $\bar{n}_{chain}$ and PDI with decreasing D_p is continued for experiments 3−5 (Table 1).

The behavior of experiment 1 is not the expected result from the reduced influence of compartmentalization in an ATRP system and necessitates further discussion. For a typical ATRP system that experiences compartmentalization effects (slower rate of polymerization, narrower PDI, higher percentage of "living" chains), as D_p increases, the influence of compartmentalization diminishes until the polymerization proceeds as it would in bulk. As such, a system capable of producing a well-controlled polymerization in bulk, which was also well-controlled when the system is compartmentalized, is expected to be well-controlled in a dispersed system containing large particles. The initiation system for this investigation (hydrogen peroxide/AA) prevents the polymerization for being conducted in bulk and attempts to create a stable latex with a D_p larger than 212 nm in experiment 1 failed (less than 0.5 wt % CTAB led to an unstable latex). However, a similar polymerization rate would indicate negligible compartmentalization effects and occurs when comparing experiment 1 with experiment 2 (Figure 1c). Although the polymerization rates are similar, experiment 2 (D_p = 176 nm) exhibits the characteristic of a well-controlled polymerization, while in experiment 1 (D_p = 212 nm) the polymerization is poorly controlled. As outlined in the pervious report,[34] the $CuBr_2$−EHA_6TREN/AA/hydrogen peroxide system exhibits significantly faster rates of polymerization (k^{app}/total number of polymer chains) than a typical miniemulsion ATRP. The conclusion was that the hydrogen peroxide/AA system yields an advantageous ratio of [Cu(I)]/[Cu(II)] that allows the polymerization to proceed at higher polymerization rates, with the reasoning that the concentration of the deactivating species ($CuBr_2$−EHA_6TREN) was regulated to very low levels by the presence of the AA. With a relatively low concentration of $CuBr_2$−EHA_6TREN, the system may only be controlled when it is compartmentalized, which is what appears to be occurring in experiments 1−5. As well, for experiments 2−5 the low number of polymer chains, with N_{chain} ranging from 730 to 2400, coupled with the compartmentalization effects, could explain how the system is capable of producing well-controlled higher polymers of much higher M_n (400 000−1 000 000 g mol^{-1}) than has previously been observed. Typically, for linear polymers produced by ATRP the M_n is limited to <200 000 g·mol^{-1}, after which the effect of the radical side reactions (termination and transfer) become significant and the livingness of the system is decreased.[37,39]

Effect of [$CuBr_2$−EHA_6TREN]$_0$. Experiments 1−5 illustrated that compartmentalization reduces the overall polymerization rate and improved control of the polymerization. Experiments 6−9 (Table 1) were run to examine the effect of [$CuBr_2$−EHA_6TREN]$_0$ on the system. The first set of experiments was run at a CTAB loading of 1 wt % (Figure 2), and the second set of experiments was conducted at a CTAB loading of 3 wt % (Figure 3). The figures show that M_n, and therefore the number of polymer chains, are not affected by [$CuBr_2$−EHA_6TREN]$_0$, which is expected since $CuBr_2$−EHA_6TREN should only deactivate propagating radicals and not influence the generation of primary radicals.

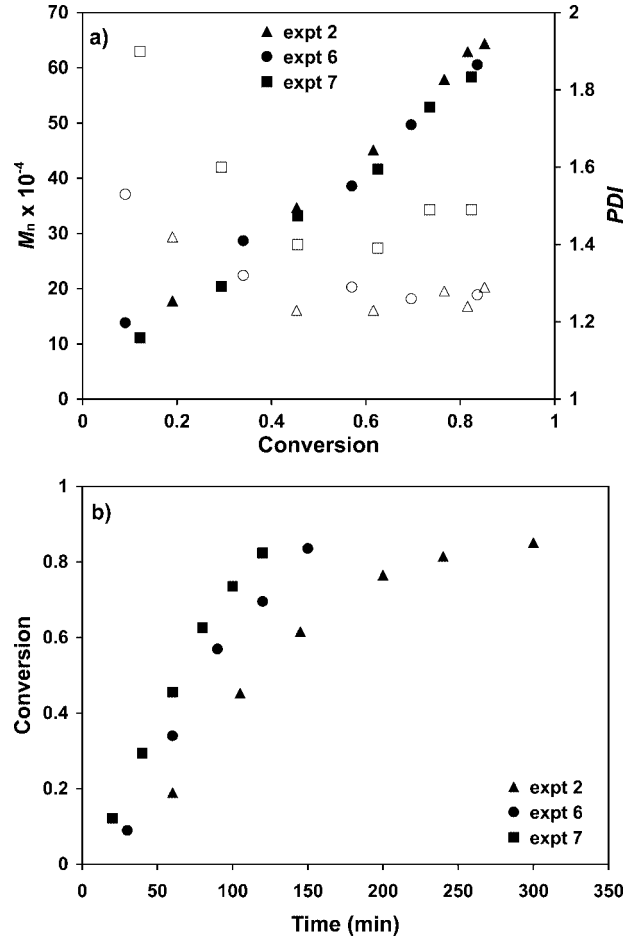

Figure 2. Evolution of (a) number-average molecular weight (M_n) and polydispersity index (PDI) with conversion and (b) conversion vs time plots for the reverse atom transfer radical polymerization of butyl methacrylate (BMA) at 90 °C in miniemulsion with 1 wt % cetyltrimethylammonium bromide, varying the [copper(II) bromide tris[2-di(2-ethylhexyl acrylate)aminoethyl]amine ($CuBr_2$−EHA_6TREN)]$_0$. 15% solid content; [hexadecane] = 3.8 wt % based on monomer; expt 2: [BMA]$_0$/[$CuBr_2$−EHA_6TREN]$_0$/[hydrogen peroxide (hydrogen peroxide)]$_0$/[ascorbic acid (AA)]$_0$ = 1270:1.6:1:0.5; expt 6: [BMA]$_0$/[$CuBr_2$−EHA_6TREN)]$_0$/[hydrogen peroxide]$_0$/[AA]$_0$ = 1270:1.3:1:0.5; expt 7: [BMA]$_0$/[$CuBr_2$−EHA_6TREN]$_0$/[hydrogen peroxide]$_0$/[AA]$_0$ = 1270:1:1:0.5.

A CTAB loading of 1 wt % produced a D_p of 176 nm for experiment 2 and ∼160 nm for experiments 6 and 7. The amount of $CuBr_2$−EHA_6TREN was progressively reduced from experiment 2 ([$CuBr_2$−EHA_6TREN]$_0$/[hydrogen peroxide]$_0$ = 1.6:1) to experiment 6 ([$CuBr_2$−EHA_6TREN]$_0$/[hydrogen peroxide]$_0$ = 1.3:1) and experiment 7 ([$CuBr_2$−EHA_6TREN]$_0$/[hydrogen peroxide]$_0$ = 1:1). In each of the experiments, the M_n grew linearly with conversion; however, the effect of decreasing [$CuBr_2$−EHA_6TREN]$_0$ can be seen in the evolution of the PDI (Figure 2a). Lowering the concentration of $CuBr_2$−EHA_6TREN was expected to reduce the level of control over the polymerization, which was seen by the PDI in experiment 7 which attains a relatively high minimum value of 1.39 at 62% conversion, before increasing to a final value of 1.49.

An identical set of experiments was run with a CTAB loading of 3 wt %, which produced a D_p of ∼119 nm. In experiment 5 ([$CuBr_2$−EHA_6TREN]$_0$/[hydrogen peroxide]$_0$ = 1.6:1), experiment 8 ([$CuBr_2$−EHA_6TREN]$_0$/[hydrogen peroxide]$_0$ = 1.3:1), and experiment 9 ([$CuBr_2$−EHA_6TREN]$_0$/[hydrogen peroxide]$_0$ = 1:1), the polymerization was well-controlled. Of significance is the comparison of the PDI evolution for experiments run with the lowest $CuBr_2$−EHA_6TREN loading, experiment 7 (PDI =

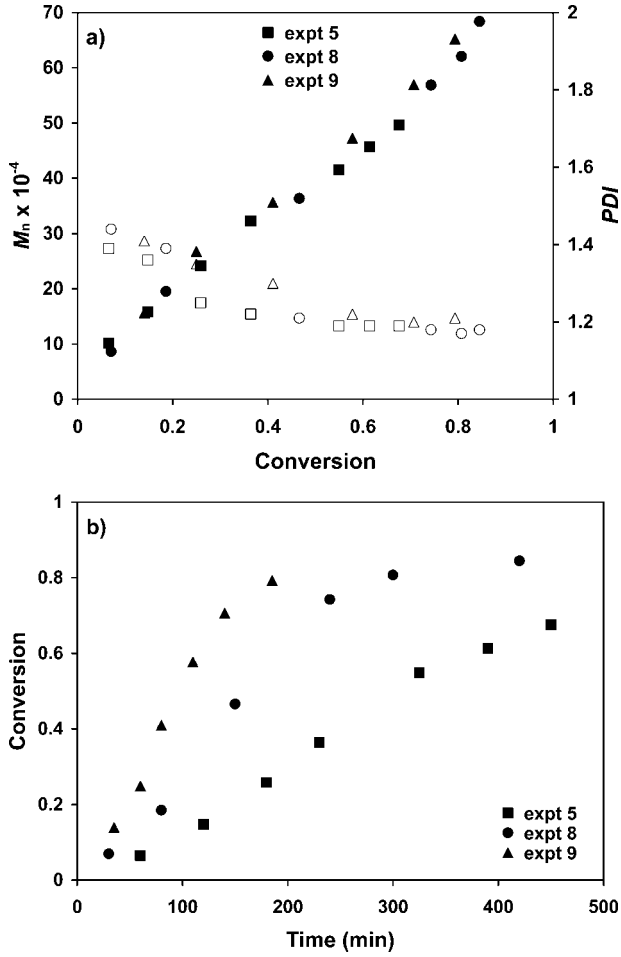

Figure 3. Evolution of (a) number-average molecular weight (M_n) and polydispersity index (PDI) with conversion and (b) conversion vs time plots for the reverse atom transfer radical polymerization of butyl methacrylate (BMA) at 90 °C in miniemulsion with 3 wt % cetyltrimethylammonium bromide, varying the [copper(II) bromide tris[2-di(2-ethylhexyl acrylate)aminoethyl]amine ($CuBr_2-EHA_6TREN$)]$_0$. 15% solid content; [hexadecane] = 3.8 wt % based on monomer; expt 5: [BMA]$_0$/$CuBr_2-EHA_6TREN$]$_0$/[hydrogen peroxide (hydrogen peroxide)]$_0$/[ascorbic acid (AA)]$_0$ = 1270:1.6:1:0.5; expt 8: [BMA]$_0$/[$CuBr_2-EHA_6TREN$)]$_0$/[hydrogen peroxide]$_0$/[AA]$_0$ = 1270:1.3:1:0.5; expt 9: [BMA]$_0$/[$CuBr_2-EHA_6TREN$]$_0$/[hydrogen peroxide]$_0$/[AA]$_0$ = 1270:1:1:0.5.

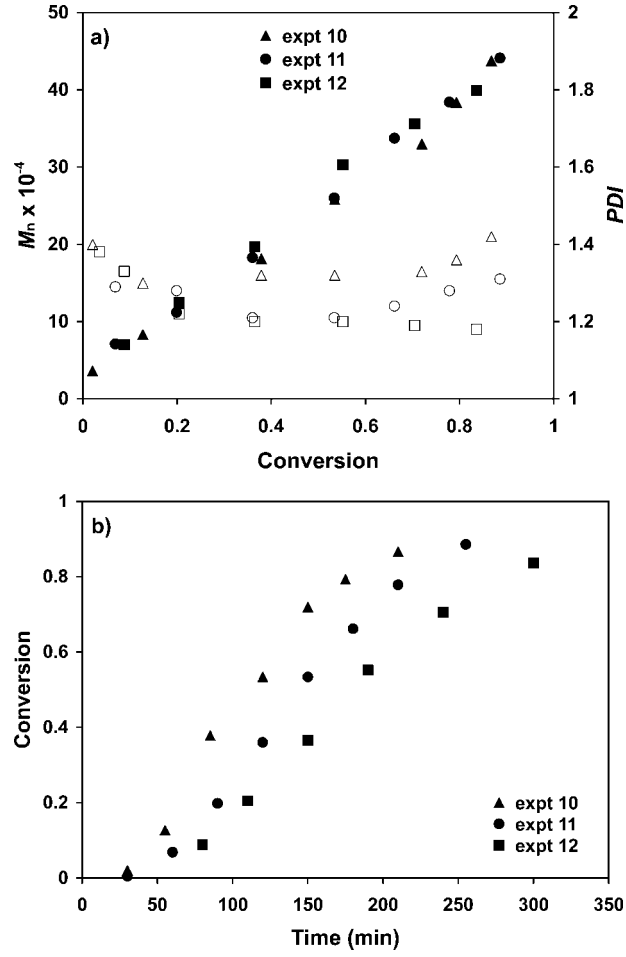

Figure 4. Evolution of (a) number-average molecular weight (M_n) and polydispersity index (PDI) with conversion and (b) conversion vs time plots for the reverse atom transfer radical polymerization of butyl methacrylate (BMA) at 90 °C in miniemulsion with varying amounts of cetyltrimethylammonium bromide (CTAB), targeting a low M_n (high number of polymer chains). 15% solid content; [hexadecane] = 3.8 wt % based on monomer; [BMA]$_0$/[copper(II) bromide tris[2-di(2-ethylhexyl acrylate)aminoethyl]amine]$_0$/[hydrogen peroxide]$_0$/[ascorbic acid]$_0$ = 630:1.6:1:0.5; expt 10: 1 wt % CTAB; expt 11: 2 wt % CTAB; expt 12: 3 wt % CTAB.

1.49) and experiment 9 (PDI = 1.21). The improved control of the polymerization in experiment 9 over experiment 7 is the result of an increased degree of compartmentalization in the system. The volume of a particle in experiment 9 (D_p = 119 nm) is ~2.4 times smaller than in experiment 7 (D_p = 159 nm).

The difference in the degree of compartmentalization between the set of experiments with 1 wt % CTAB and 3 wt % CTAB is apparent from the conversion vs time profiles (Figure 2b and Figure 3b). The figures illustrate that with 3 wt % CTAB the polymerizations are significantly slower than the runs stabilized with only 1 wt % CTAB. This can also be seen comparing the k^{app}, which are greater for the 1 wt % CTAB experiments (19.2 × 10^5, 23.3 × 10^5, and 29.2 × 10^5 s^{-1} for experiments 2, 6, and 7, respectively) than the experiments conducted with 3 wt % CTAB (5.0 × 10^5, 11.3 × 10^5, and 17.3 × 10^5 s^{-1} for experiments 5, 8, and 9, respectively).

Effect of Target M_n (Number of Chains). Since it was argued that compartmentalization stemmed from the low number of polymer chains per particle (thereby limiting the concentration of active polymeric radicals and $CuBr_2-EHA_6TREN$), it was of interest to see what influence the number of chains (controlled by the target M_n) would have on the polymerization. In the first set of experiments (experiments 10−12) the number of polymer chains was increased by reducing the [BMA]$_0$/[$CuBr_2-EHA_6TREN$]$_0$/[hydrogen peroxide]$_0$ ratio from 1270:1.6:1 to 630:1.6:1. The decrease in M_n was slightly less than the factor of 2 expected (indicating a greater efficiency for chain initiation in experiments 10−12). The plots of M_n and PDI vs conversion are displayed in Figure 4a. All the polymerizations were controlled, with the M_n increasing linearly with conversion and the PDI remaining low. For experiment 10 (D_p = 172 nm, PDI = 1.42) and experiment 11 (D_p = 147 nm, PDI = 1.31) the PDI did increase with conversion after ~60% conversion, and the final PDI was relatively high compared to experiment 12 (D_p = 130 nm, PDI = 1.18), a trend that is rationalized by compartmentalization effects. When the concentration of polymer chains in the system is increased (experiments 10−12) from the levels in experiments 2−5, there is an increase in the final PDI of the polymer formed, with the exception of experiment 12 (3 wt % CTAB). The PDI of 1.18 in experiment 12 confirms that the difference in the PDI for the experiments with a high concentration of polymer chain vs a low concentration of polymer chains cannot be attributed to the expected trend in an ATRP system of a decrease in PDI with higher M_n. Instead, the greater PDI is attributed to the higher N_{chain} which serves

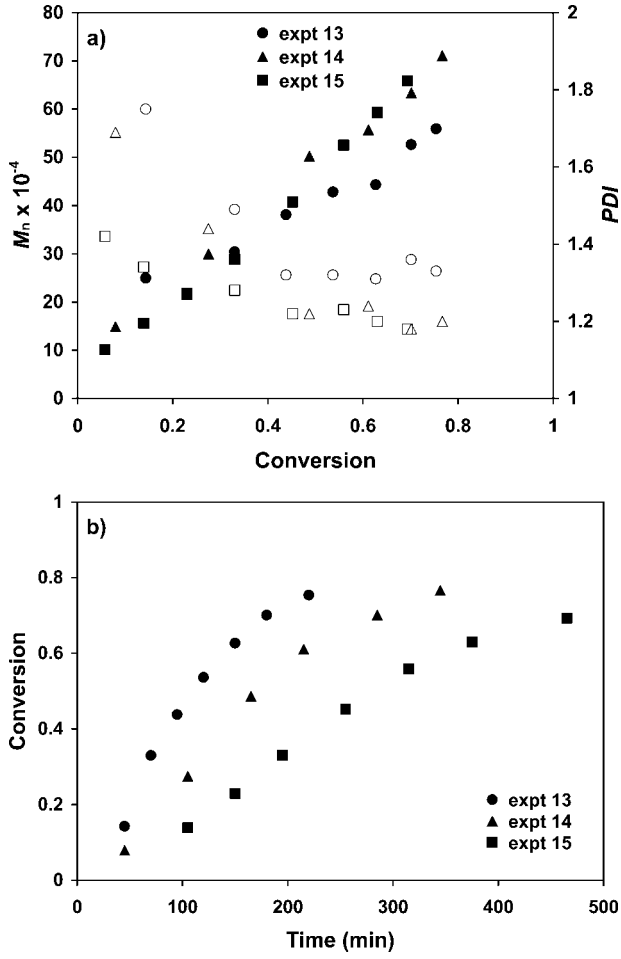

Figure 5. Evolution of (a) number-average molecular weight (M_n) and polydispersity index (PDI) with conversion and (b) conversion vs time plots for the reverse atom transfer radical polymerization of butyl methacrylate (BMA) at 90 °C in miniemulsion with varying amounts of cetyltrimethylammonium bromide (CTAB), targeting a high M_n (low number of polymer chains). 15% solid content; [hexadecane] = 3.8 wt % based on monomer; $[BMA]_0/[copper(II)\ bromide\ tris[2\text{-}di(2\text{-}ethylhexyl\ acrylate)aminoethyl]amine]_0/[hydrogen\ peroxide]_0/[ascorbic\ acid]_0$ = 1590:1.6:1:0.5; expt 13: 1 wt % CTAB; expt 14: 2 wt % CTAB; expt 15: 3 wt % CTAB.

to reduce compartmentalization effects in the system. This was observed by the conversion vs time profiles of Figure 4b and the k^{app} values in Table 1 for experiments 10−12 that have a significantly narrower range than for experiments 2−5 that had the higher degree of compartmentalization. It could also be seen in the small effect that D_p had on the value of $\bar{n}_{chain}$ (ranging from 6.8×10^{-6} to 4.5×10^{-6} L_{water}^{-1} $chain^{-1}$) for experiments 10−12 compared with the large variation of $\bar{n}_{chain}$ (from 10.3×10^{-6} to 2.7×10^{-6} L_{water}^{-1} $chain^{-1}$) for the system with a lower chain concentration (experiments 2−5).

If a higher concentration of reactants reduces the impact of compartmentalization, then a polymerization with a lower concentration of reactants would be expected to exhibit a greater influence due to compartmentalization. In the set of experiments 13−15, the number of polymer chains was decreased by increasing the $[BMA]_0/[CuBr_2-EHA_6TREN]_0/[hydrogen\ peroxide]_0$ ratio from 1270:1.6:1 to 1590:1.6:1, resulting in a proportional increase in M_n. From Figure 5a, the M_n increased linearly with conversion, and the PDI decreased with conversion. The expected compartmentalization trends are seen in the conversion vs time profiles in Figure 5b, which depicts the slower polymerization rate with decreasing D_p. As well, the kinetic data in Table 1 reveals a decrease in k^{app} and $\bar{n}_{chain}$ with D_p. In agreement with the previous results, experiment 13 (with the largest D_p of 155 nm) exhibited the lowest control over the polymerization. Accompanying the relatively high PDI of 1.33 was also a large increase in molecular weight at the beginning of the reaction (M_n = 249 800 g mol^{-1} at 14% conversion). After the initial increase, the M_n grew linearly with conversion; however, the final M_n (∼560 000 g mol^{-1} at 75% conversion) was significantly lower than in experiments 14 and 15 (M_n = ∼ 700 000 g mol^{-1} at 75% conversion). The large increase in M_n in the early stages of the polymerization suggests a lack of $CuBr_2-EHA_6TREN$ to mediate the polymerization; however, with the same formulation, experiments 14 (2 wt % CTAB D_p = 131 nm) and 15 (3 wt % CTAB, D_p = 117 nm) show significantly better control over the polymerization. It is believed that in the larger reaction volume of experiment 13 the $CuBr_2-EHA_6TREN$ cannot effectively mediate the active radicals (which are at their peak concentration at the beginning of the polymerization), causing the polymerization to proceed rapidly with poorer control.

Conclusions

The results from these experiments have shown that compartmentalization can influence miniemulsion reverse ATRP under the right set of conditions. Compartmentalization of an ATRP system requires that the probability of having two active chains in one particle becomes sufficiently low that varying the particle size alters the number of active radicals (through segregation and confined space effects). This probability is determined by both the particle volume and the number of polymer chains within each particle. The value of N_{chain} is important in miniemulsion ATRP because compartmentalization effects (at a given particle volume) will only be evident if the number of reactants (active polymeric radicals and the deactivator $CuBr_2-EHA_6TREN$) is limited by the available volume of the particle. This was confirmed with systems having N_{chain} > 10 000 chains/particle that showed no evidence of compartmentalization and explains why compartmentalization has not been previously seen in aqueous-based ATRP systems.

Compartmentalization was found to reduce the overall polymerization rate, likely due to an increasing rate of deactivation due to the confined space effect. More significantly, however, compartmentalization also improves the control over the polymerization and reduces the final PDI of the polymer.

The differences between a conventional free radical polymerization and ATRP are highlighted by the opposing impact that compartmentalization has on the kinetics of the polymerizations. In a conventional system, radical segregation causes an increase in the polymerization rate, while the confined space effect in ATRP dominates the kinetics and causes a reduction in the polymerization rate. Decreasing particle volume increases the reaction rate between an active polymeric radical and the persistent radical species, $CuBr_2-EHA_6TREN$, lowering the value of $\bar{n}_{chain}$.

Both radical segregation and the confined space effect improve control over the polymerization. Increased compartmentalization was shown to improve the linearity of growth of M_n with conversion, decrease the PDI of the polymer, and maintain better control of the polymerization during the early stage of the polymerization when the radical concentration is at its peak value.

References and Notes

(1) Cunningham, M. F. *Prog. Polym. Sci.* **2002**, *27*, 1039–1067.
(2) Qiu, J.; Charleux, B.; Matyjaszewski, K. *Prog. Polym. Sci.* **2001**, *26*, 2083–2134.
(3) Cunningham, M. F. *Prog. Polym. Sci.* **2008**, *33*, 365–398.
(4) Matyjaszewski, K.; Shipp, D. A.; Qiu, J.; Gaynor, S. G. *Macromolecules* **2000**, *33*, 2296–2298.

(5) Qiu, J.; Pintauer, T.; Gaynor, S. G.; Matyjaszewski, K.; Charleux, B.; Vairon, J.-P. *Macromolecules* **2000**, *33*, 7310–7320.
(6) Li, M.; Matyjaszewski, K. *J. Polym. Sci., Part A: Polym. Chem.* **2003**, *41*, 3606–3614.
(7) Li, M.; Matyjaszewski, K. *Macromolecules* **2003**, *36*, 6028–6035.
(8) Li, M.; Min, K.; Matyjaszewski, K. *Macromolecules* **2004**, *37*, 2106–2112.
(9) Li, M.; Jahed, N. M.; Min, K.; Matyjaszewski, K. *Macromolecules* **2004**, *37*, 2434–2441.
(10) Min, K.; Gao, H.; Matyjaszewski, K. *J. Am. Chem. Soc.* **2005**, *127*, 3825–3830.
(11) Kagawa, Y.; Zetterlund, P. B.; Minami, H.; Okubo, M. *Macromolecules* **2007**, *40*, 3062–3069.
(12) Simms, R. W.; Cunningham, M. F. *J. Polym. Sci., Part A: Polym. Chem.* **2006**, *44*, 1628–1634.
(13) Farcet, C.; Lansalot, M.; Charleux, B.; Pirri, R.; Vairon, J. P. *Macromolecules* **2000**, *33*, 8559–8570.
(14) Farcet, C.; Nicolas, J.; Charleux, B. *J. Polym. Sci., Part A: Polym. Chem.* **2002**, *40*, 4410–4420.
(15) Pan, G.; Sudol, E. D.; Dimonie, V. L.; El-Aasser, M. S. *Macromolecules* **2002**, *35*, 6915–6919.
(16) Cunningham, M. F. *C. R. Chim.* **2003**, *6*, 1351–1374.
(17) Pan, G.; Sudol, E. D.; Dimonie, V. L.; El-Aasser, M. S. *J. Polym. Sci., Part A: Polym. Chem.* **2004**, *42*, 4921–4932.
(18) Saka, Y.; Zetterlund, P. B.; Okubo, M. *Polymer* **2007**, *48*, 1229–1236.
(19) Gilbert R. G. *Emulsion Polymerization—A Mechanistic Approach*; Academic Press: New York, 1995.000
(20) Butte, A.; Storti, G.; Morbidelli, M. *Macromolecules* **2000**, *33*, 3485–3487.
(21) Monteiro, M. J.; Hodgson, M.; De Brouwer, H. *J. Polym. Sci., Part A: Polym. Chem.* **2000**, *38*, 3864–3874.
(22) Monteiro, M. J.; de Barbeyrac, J. *Macromolecules* **2001**, *34*, 4416−4423.
(23) Butte, A.; Storti, G.; Morbidelli, M. *Macromolecules* **2001**, *34*, 5885−5896.
(24) Prescott, S. W. *Macromolecules* **2003**, *36*, 9608–9621.
(25) Charleux, B. *Macromolecules* **2000**, *33*, 5358–5365.
(26) Butte, A.; Storti, M.; Morbidelli, M. *DECHEMA Monogr.* **1998**, *134*, 497–507.
(27) Zetterlund, P. B.; Okubo, M. *Macromolecules* **2006**, *39*, 8959–8967.
(28) Nakamura, T.; Zetterlund, P. B.; Okubo, M. *Macromol. Rapid Commun.* **2006**, *27*, 2014–2018.
(29) Maehata, H.; Buragina, C.; Cunningham, M.; Keoshkerian, B. *Macromolecules* **2007**, *40*, 7126–7131.
(30) Delaittre, G.; Charleux, B. *Macromolecules* **2008**, *41*, 2361–2367.
(31) Kagawa, Y.; Zetterlund, P. B.; Minami, H.; Okubo, M. *Macromol. Theory Simul.* **2006**, *15*, 608–613.
(32) Klee, J. E.; Neidhart, F.; Flammersheim, H.-J.; Mülhaupt, R. *Macromol. Chem. Phys.* **1999**, *200*, 517–523.
(33) Zeng, F.; Shen, Y.; Zhu, S.; Pelton, R. *Macromolecules* **2000**, *33*, 1628–1635.
(34) Simms, R. W.; Cunningham, M. F. *Macromolecules* **2007**, *40*, 860–866.
(35) Beuermann, S.; Buback, M.; Davis, T. P.; Gilbert, R. G.; Hutchinson, R. A.; Kajiwara, A.; Klumperman, B.; Russell, G. T. *Macromol. Chem. Phys.* **2000**, *201*, 1355–1364.
(36) Matyjaszewski, K.; Patten, T. E.; Xia, J. *J. Am. Chem. Soc.* **1997**, *119*, 674–680.
(37) Matyjaszewski, K.; Xia, J. *Chem. Rev.* **2001**, *101*, 2921–2990.
(38) Zhang, H.; Klumperman, B.; Ming, W.; Fischer, H.; van der Linde, R. *Macromolecules* **2001**, *34*, 6169–6173.
(39) Kamigaito, M.; Ando, T.; Sawamoto, M. *Chem. Rev.* **2001**, *101*, 3689–3745.

MA8003967